Journal of Alloys and Compounds 695 (2017) 1301–1306

Contents lists available at ScienceDirect

Journal of Alloys and Compounds

journal homepage: http://www.elsevier.com/locate/jalcom

The experiment and theory studies of silver substituting cadmium in CdS quantum dots

Jianbo Yin [a, b, *], Xuefeng Lu [b], Qizheng Dong [b]

[a] State Key Laboratory of Advanced Processing and Recycling of Non–ferrous Metals, Lanzhou University of Technology, Lanzhou, 730050, China
[b] School of Material Science and Engineering, Lanzhou University of Technology, Lanzhou, 730050, China

ARTICLE INFO

Article history:
Received 10 August 2016
Received in revised form
20 October 2016
Accepted 27 October 2016
Available online 2 November 2016

Keywords:
Cadmium sulfide
Luminescence
Nanoparticles
Silver

ABSTRACT

This paper reports the experiment and theory simulation results of silver substituting cadmium in CdS quantum dots (QDs). The experiment results show that the average particle size of as-prepared samples is about 6.0 nm, and the phase structure is hexagonal wurtzite. Compared with that of pure CdS QDs, the peak of photoluminescence spectrum of CdS QDs the cadmium of which are substituted by silver are red shift from 533 nm to 567 nm, which leads to the luminous colours change from green to yellow. The theoretical simulation results show that the optical property changes of CdS QDs are due to the silver substituting cadmium changing the energy level spacing, the conductivity and the way of electronic transition of CdS crystals.

1. Introduction

Quantum dots (QDs) show unique physical properties that make them a widely studied material for applications in several fields such as photonics, optoelectronics, and biotechnology [1–4]. CdS based QDs have been the workhorse for these applications in the past decade due to their excellent physical and chemical properties [5–7]. Recently, attention has been paid on the synthesis of colour-tunable CdS QDs emitters with high extinction coefficients. For example, Schneider and his coworkers synthesized CdS QDs with different colours by capped route [8], Chen and his coworkers constructed highly luminescent CdTe/CdS @ ZnS–SiO_2 QDs by surface adsorption routes [9]. However, element substitution reaction is rarely adopted to change the physical properties of CdS QDs due to it is hard to find a proper method, and it also seems a difficult work to achieve under the dimension of the QDs. Therefore, we transplanted microemulsion-mediated hydrothermal route which is a simple method often used in the preparation of quantum dots [10,11] to synthesize CdS QDs of silver substituting cadmium, the purpose of which is to give an example of doping materials with a new method.

Furthermore, in order to study the optical properties change mechanism of CdS QDs the cadmium of which is substituted by silver, theoretical simulation calculation is adopted to support the experiment results. The first principle calculation, which starts from the specific requirements, is a very powerful tool to investigate the microscopic property of a semiconductor [12–14]. It is an approximation algorithm of direct solving Schrodinger equation by using the density functional theory (DFT) of quantum mechanics according to the principle of atomic nuclei and electrons interaction with each other and the basic law of motion. Usually, researchers adopt the local density approximation (LDA) or generalized gradient approximation (GGA) functional to simulate the band structure of a semiconductor [15,16], but the results are often underestimated, and the simulated band gap of CdS is about 1.0 eV [17,18], which is often doubted by the researchers of experiments. This underestimation of band gap is mainly related to the inherent lack of derivative discontinuity and delocalization error in the exchange-correlation functional derivative [19,20]. The hybrid B3LYP functional which means Becke three-parameter, Lee-Yang-Parr, can generally give more accurate band gap values and more precise description of electronic structures of semiconductors, and it provides a perfect way to simulate the band structure to reveal the property change mechanism of a semiconductor [21–23].

Therefore, in this paper, silver is chosen as the substitution element in CdS QDs and B3LYP is chosen as the functional to simulate the band structure and density of state of that, the purpose

* Corresponding author. State Key Laboratory of Advanced Processing and Recycling of Non–ferrous Metals, Lanzhou University of Technology, Lanzhou, 730050, China.
E-mail addresses: jianbery@163.com (J. Yin), dongqzh@163.com (Q. Dong).

http://dx.doi.org/10.1016/j.jallcom.2016.10.260
0925-8388/

of which is to offer mechanism explanations for the experiment results.

2. Experiments and computational details

2.1. Experiments

Firstly, cadmium acetate ($Cd(OAc)_2 \cdot 2H_2O$, 0.005 M) was dissolved in deionized water with magnetic stirring; secondly, the aqueous solution of thioacetamide (CH_3CSNH_2, 0.005 M) and a small amount of silver nitrate ($AgNO_3$, 3.9×10^{-5} M) was also prepared by the same process. Then, two types of reverse microemulsion (M-Cd and M-S-Ag) with aqueous phases were prepared. Both M-Cd and M-S-Ag contained three common components: a surfactant of cetyltrimethylammonium bromide ($C_{19}H_{42}BrN$), a cosurfactant of n-butyl alcohol ($CH_3CH_2CH_2CH_2OH$) and a continuous oil phase of n-hexane (C_6H_{14}), the volume ratio of which is 3:5:20. After mixing together with continuous stirring at room temperature for 30 min, they were transferred into a 50 mL Teflon-lined autoclave with hydrothermal treatment at 100 °C for 6 h, followed by cooling to room temperature naturally. The orange precipitates were separated from the reaction media by centrifugation, washed with anhydrous ethanol and deionized water several times and then dried at 70 °C. Finally, CdS QDs of silver substituting cadmium were obtained.

2.2. Characterization

The crystal structure was characterized by a Bruker D8 Advance X-ray diffractometer with Cu Kα radiation. The morphology was analyzed with a transmission electronmicroscope (TEM, TECNAI G^2 TF20). The particle size was analyzed by Mastersizer 3000 laser particle size analyzer. The optical properties of the as-prepared samples were characterized by the UV-4100 spectrophotometer and F 97 fluorospectrometer.

2.3. Computational details

The first principle calculation of CdS QDs of silver substituting cadmium was carried out with the Cambridge Serial Tatal Energy Package module (CASTP) of material studio 6.0 version. The calculations adopted supercell of hexagonal wurtzite CdS, which consists 8 atoms, including 4 cadmium atoms and 4 sulfur atoms as shown in Fig. 1. The core electrons were optimized by the norm-conserving pseudopotentials and PBE functional. The B3LYP mode was chosen for the functional of band gap calculation. The exchange-correlation effects of valence electrons were described through the B3LYP hybrid density functional and Perdew-Burke-Ernzerhof (PBE). The Monkhorst-Pack scheme k-points grid sampling was set as $4 \times 4 \times 2$ for the irreducible Brillouin zone, and the energy cutoff was set as 450 eV. The electronic configurations are $4d^{10}5s^2$ for cadmium, $4s^24p^64d^{10}5s^1$ for silver and $3s^23p^4$ for sulfur.

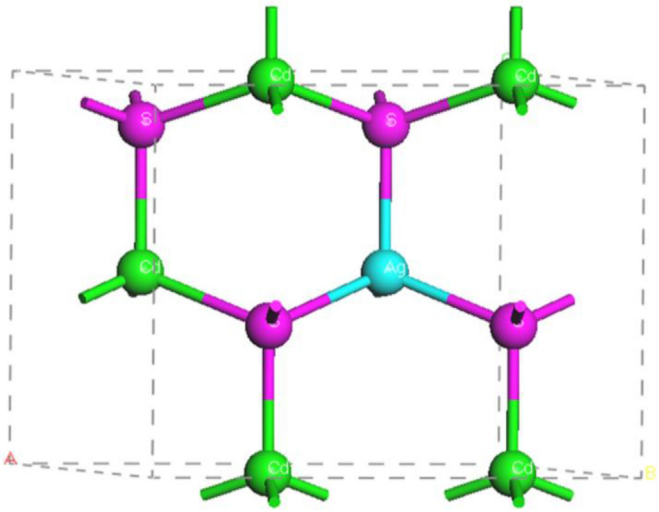

Fig. 1. Supercell of CdS of silver substituting cadmium.

3. Results and discussion

Fig. 2 shows the characterization results of CdS QDs of silver substituting cadmium. Fig. 2a shows the TEM image of monodispersed pure CdS QDs the size range of which is about 4–8 nm, and it coincides with the result of the laser particle size analyzer (Fig. 2c) which shows that the average diameter is 6 nm. From the inset section (HRTEM image), it can be seen that the lattice fringes with an interplanar distance of about 0.312 nm is the characteristic fringe spacing of the hexagonal wurtzite CdS crystal phase in the (101) plane. In contrast with that of CdS QDs, the morphology of CdS QDs of silver substituting cadmium (Fig. 2b and d) synthesized by the same route shows no difference with that of pure CdS QDs, indicating that the introduction of silver atoms don't change the crystal structure of hexagonal wurtzite CdS due to the ratio of silver is very small and the atom radius of cadmium (1.71 Å) and silver (1.75 Å) are similar which is also the reason why silver is chosen as the substitution element.

Fig. 3a shows the XRD pattern of the as prepared pure CdS QDs. The wide diffraction peaks indicate that the samples are nanocrystals. All the diffraction peaks can be indexed as hexagonal wurtzite CdS (The lattice constant of $a = b = 4.136$ Å and $c = 6.713$ Å), which are in good agreement with the value of JCPDS Card (No. 77-2306). Compared with that of pure CdS QDs, the XRD pattern of the as prepared CdS QDs of silver substituting cadmium doesn't change significantly, which indicates that the small amount of Ag doesn't cause any change of the crystal structure. Also, no other peaks of impurities were detected, revealing high purity of the as-prepared samples.

Fig. 4 shows the surface element scanning results of CdS QDs of silver substituting cadmium through EDS characterization. Fig. 4a is the STEM image of the as prepared CdS QDs of silver substituting cadmium, which points out the scanning area. The element scanning results are shown in Fig. 4b–f, respectively. It can be seen that the element distribution of Cd and S are in Fig. 4b–d, respectively. The well-distributed element scanning maps of Ag is shown in Fig. 4e and f, respectively; because the electron penetration distance of EDS is about 1.0 μm, the results indicate that the CdS QDs of silver substituting cadmium are well-distributed. Therefore, the element analysis results show that the microemulsion-mediated hydrothermal method can achieve well distributed silver doping CdS QDs.

Fig. 5 shows the absorption spectrum of CdS QDs of silver substituting cadmium. It can be seen from the absorption curves that Fig. 5b has a distinct blue shift compared with that of Fig. 5a, indicating that the introduction of Ag can lead to structural defects of CdS QDs which cause the absorption curve blue shift.

Fig. 6 shows the photoluminescence emission spectrum of CdS QDs of silver substituting cadmium. It can be seen that the emission peak of CdS QDs (Fig. 6a) is at 533 nm, which means the emission light is green. The emission peak of CdS QDs of silver substituting cadmium (Fig. 6b) is at 567 nm, which means the emission light is yellow. Therefore, the results show that the introduction of Ag in CdS QDs leads to the emission peak red shifts for 34 nm.

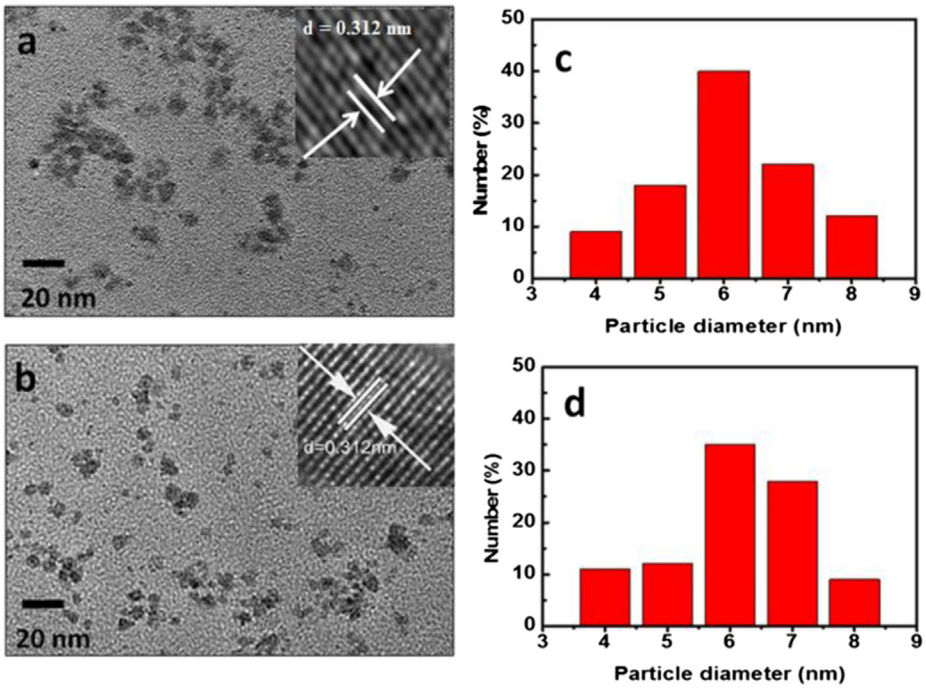

Fig. 2. TEM images of CdS QDs (a) and CdS QDs of silver substituting cadmium (b). (c) and (d) are the corresponding size distribution histograms.

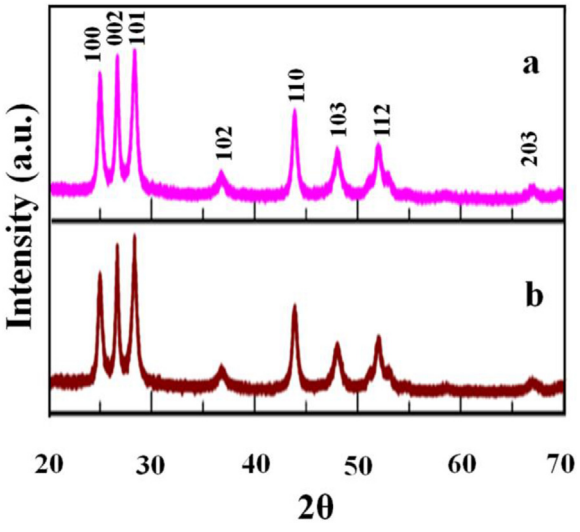

Fig. 3. XRD patterns of CdS QDs (a) and CdS QDs of silver substituting cadmium (b).

In order to study the optical properties change mechanism of Figs. 5 and 6, the first principle is adopted to simulate the band structure of silver substituting cadmium CdS. The space group of hexagonal wurtzite CdS of silver substituting cadmium adopted by the simulation is $P6_3mc$. The lattice parameters of hexagonal wurtzite CdS crystal are a = b = 4.121 Å, c = 6.682 Å, $\alpha = \beta = 90^\circ$ and $\gamma = 120^\circ$. In order to obtain a stable crystal structure, the optimized calculation of lattice parameter is carried out using the parameter above. The lattice parameters after optimized calculation are a = b = 4.203 Å, c = 6.691 Å, and the maximum deviation of the optimized crystal lattice constants is 2.0%, showing that the accuracy of the built crystal cell is very high.

The simulated band structure of hexagonal wurtzite CdS along the high symmetry direction in the Brillouin zone is based on the hybrid B3LYP functional, and the results are shown in Fig. 7a. The Fermi level indicated by red line is set to zero. Both the valence band maximum and conduction band minimum of CdS are in the same line (G line), indicating hexagonal wurtzite CdS is a direct band gap semiconductor. The calculated band gap value (from Fermi level to minimum of the conduction band) is 2.79 eV, which is closed to the value of experiment (2.54 eV), and most of the calculated value reported by the literature is 1.0 eV [15,16], indicating the results calculated by us are more accurately. Therefore, it concludes that the calculation method which chosen by us is appropriate. Fig. 8a shows the density of states (DOS) of hexagonal wurtzite CdS. It can be seen from the top of valence band (−4 to 0 eV) that the electron density mainly consists of the bonding state of Cd−s and S−p, and from the bottom of conduction band (0−4 eV), it can be seen that the electron density mainly includes the bonding state of Cd−s and S−s. Therefore, it can be concluded that the valence band maximum is mainly determined by the bonding state of Cd−s and S−p interaction and the conduction band minimum is mainly determined by the bonding state of Cd−s and S−s interaction. Fig. 7b shows the band structure of hexagonal wurtzite CdS of silver substituting cadmium. The introduction of Ag element in CdS crystal can lead to the impurity levels of conduction band, the reason of which is Ag (+1) has a different chemical valence with that of cadmium (+2), and they have different arrangement of extranuclear electrons. It can be seen that the band gap is still 2.79 eV, and it doesn't changed, but the energy level spacing changes obviously compared with that of pure CdS, and the impurity level bends across the Fermi level, which shows the conductivity characteristics, and it can enhance the electroconductivity of the sample. That can be also proved by Fig. 8b, from which it can be seen that the total density has changed. And the impurity levels are caused by the bonding state of S−p and Ag−p interaction (0−4 eV), indicating that the doping of Ag can change the valence band structure of CdS. This can change the way of electronic transition from valence band to conduction band and conductivity of CdS. The electron transition can be from impurity

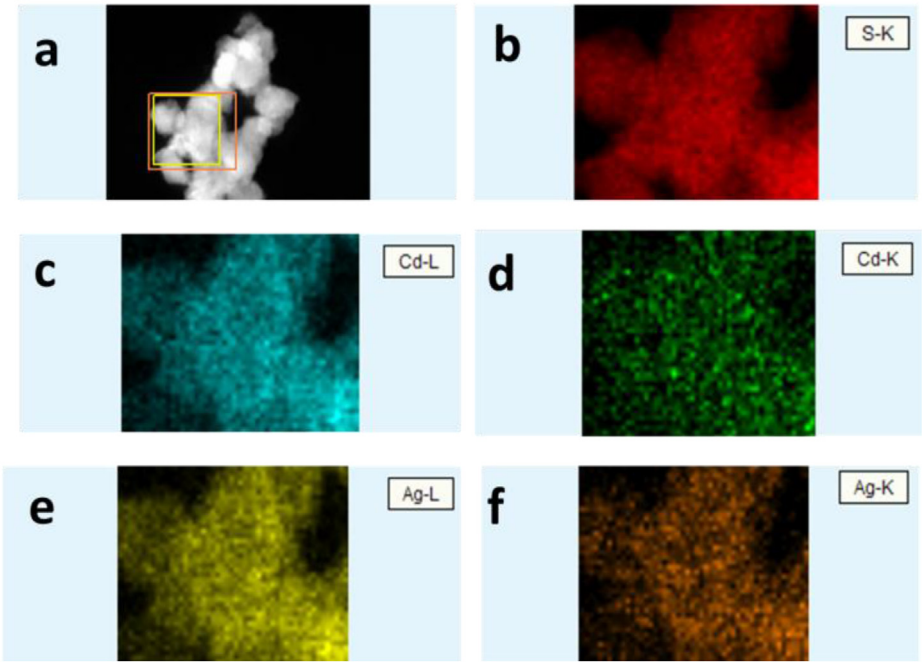

Fig. 4. STEM image (a) and element analysis results (b–f) of CdS QDs of silver substituting cadmium.

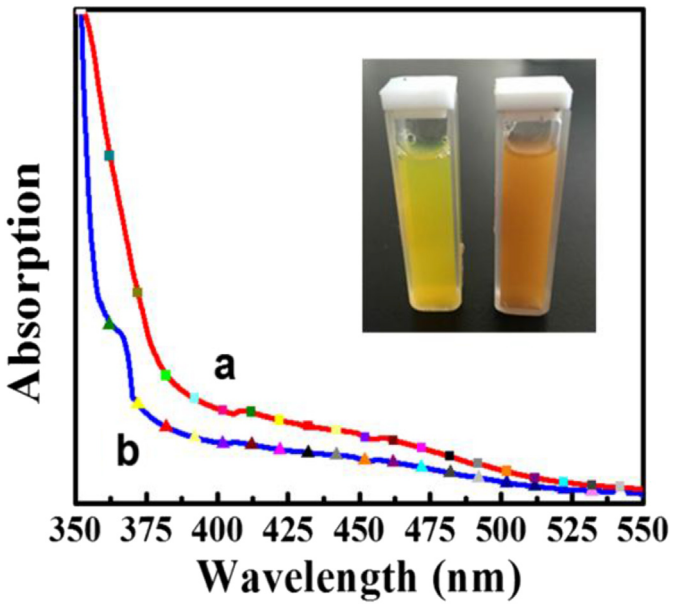

Fig. 5. Absorption spectra of CdS QDs (a) and CdS QDs of silver substituting cadmium (b).

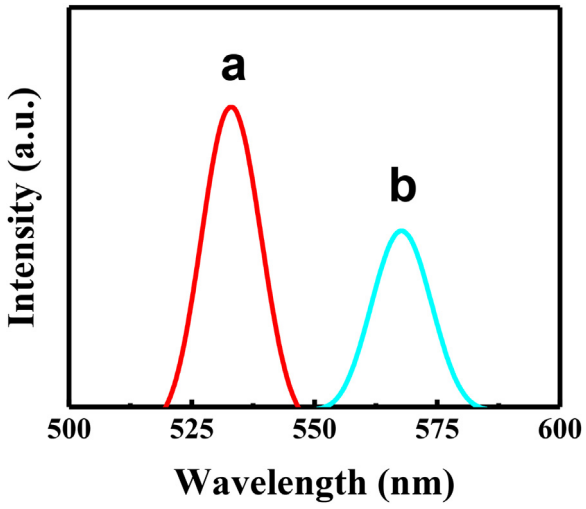

Fig. 6. Photoluminescence spectra of CdS QDs (a) and CdS QDs of silver substituting cadmium (b).

levels to conduction band which can close the distance of that. Therefore, the simulated results show that absorption and photoluminescence spectra changes of the experiments are caused by the changes of energy level spacing, the conductivity and the way of electronic transition of CdS atom. The synthetic action of energy level spacing, the way of electronic transition and the conductivity changes may lead to the changes of photoluminescence colour and intensity (Fig. 6). The way of electronic transition change results in the blue shift of the absorption curves (Fig. 5).

4. Conclusions

In summary, silver is chosen as the substitution element of CdS QDs to change the optical property. The experiment results show that the average particle size of the as-prepared sample is about 6.0 nm, and they are hexagonal wurtzite phase. Compared with CdS QDs, the photoluminescence emission peaks of CdS QDs are red shift from 533 nm to 567 nm, which leads to the emission colours change from green to yellow. The simulation results show that the optical property change is caused by the synthetic action of the energy level spacing, the conductivity and the way of electronic transition changes of CdS crystals.

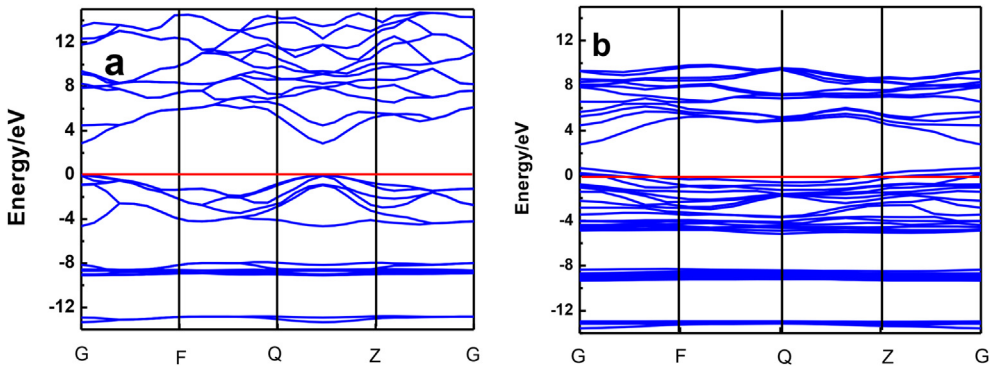

Fig. 7. The band structure maps of pure wurtzite CdS (a) and CdS QDs of silver substituting cadmium (b).

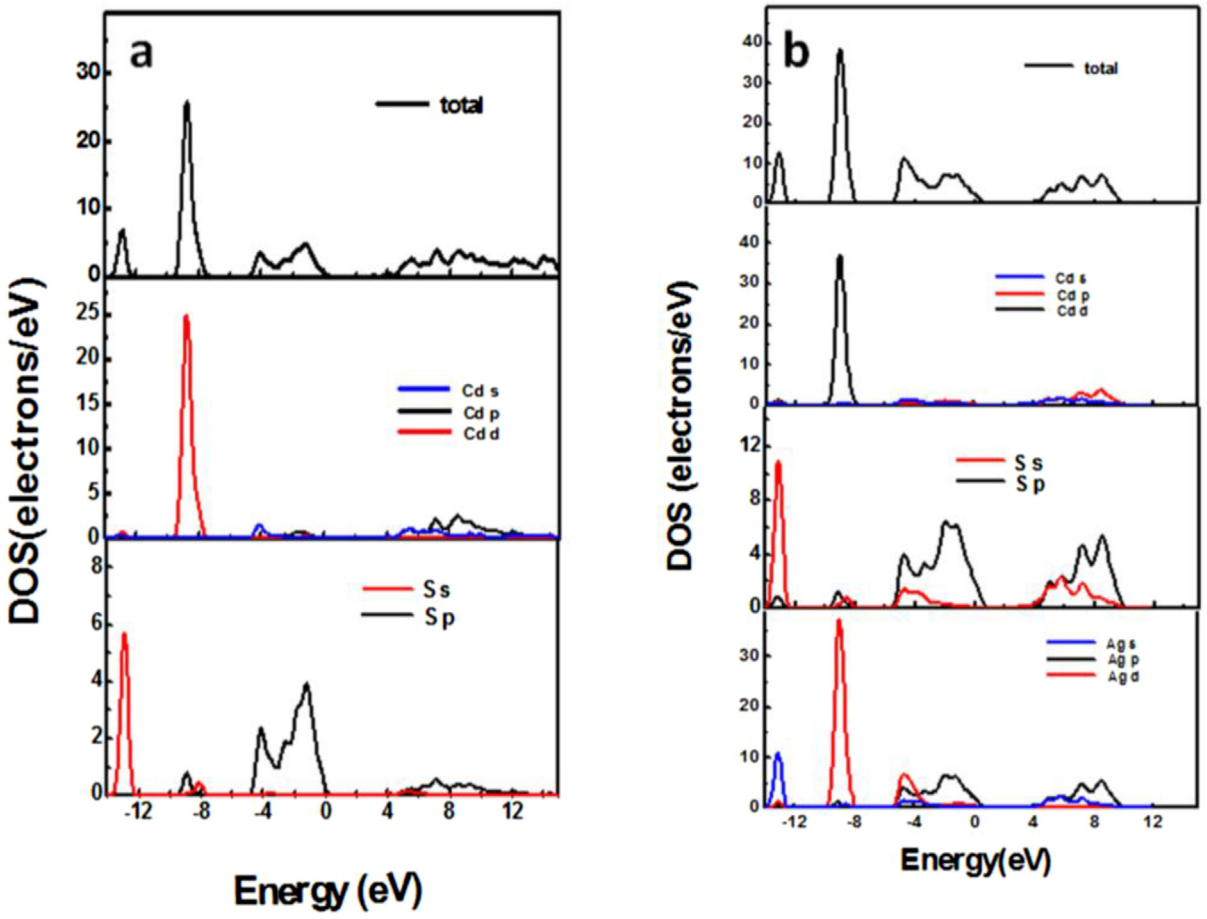

Fig. 8. Density of state maps of pure wurtzite CdS (a) and CdS QDs of silver substituting cadmium (b).

Acknowledgment

This paper is supported by the Gansu Provincial Youth Science and Technology Fund Projects (1506RJYA093) and National Natural Science Foundations of China (Granted No. 51402142 and No. 21301084 and No. 51662026).

References

[1] J. Zhou, Y. Yang, C. Zhang, Chem. Rev. 115 (2015) 11669–11717.
[2] G.H. Carey, A.L. Abdelhady, Z. Ning, S.M. Thon, O.M. Bakr, E.H. Sargent, Chem. Rev. 115 (2015) 12732–12763.
[3] C. Zhou, Y. Geng, Q. Chen, J. Xu, N. Huang, Y. Gan, L. Zhou, Mater. Lett. 172 (2016) 171–174.
[4] J. Zhang, W. Sun, L. Yin, X. Miao, D. Zhang, J. Mater. Chem. C 2 (2014) 4812–4817.
[5] L. Liu, J. Hui, L. Su, J. Lv, Y. Wu, J.T.S. Irvine, Mater. Lett. 132 (2014) 231–235.
[6] U.T.D. Thuy, L.A. Tu, N.T. Loan, T.T.K. Chi, N.Q. Liem, Opt. Mater 53 (2016) 34–38.
[7] Z. Deng, P. Guyot-Sionnest, ACS Nano 10 (2016) 2121–2127.
[8] A. Aboulaich, D. Billaud, M. Abyan, L. Balan, J.J. Gaumet, G. Medjadhi, J. Ghanbaja, R. Schneider, ACS Appl. Mater. Interfac. 4 (2012) 2561–2569.
[9] L.H. Mao, Q.H. Zhang, Y. Zhang, C.F. Wang, S. Chen, Ind. Eng. Chem. Res. 53 (2014) 16763–16770.
[10] R. Chen, B. Han, L. Yang, Y. Yang, Y. Xu, Y. Mai, J. Luminesce 172 (2016) 197–200.
[11] L. Yang, L. Liu, D. Xiao, J. Zhu, Mater. Lett. 72 (2012) 113–115.
[12] D. Guo, H. Hua, Q. Yang, X. Li, C. Hu, J. Phys. Chem. C 118 (2014) 11426–11431.

[13] G.B. Liu, D. Xiao, Y. Yao, X. Xu, W. Yao, Chem. Soc. Rev. 44 (2015) 2643–2663.
[14] H. Fang, H. Demir, P. Kamakoti, D.S. Sholl, J. Mater. Chem. A 2 (2014) 274–291.
[15] J. Yin, X. Lu, Q. Dong, Compu. Mater. Sci. 122 (2016) 86–91.
[16] J. Yin, X. Lu, Q. Dong, J. Alloy, Compoun 678 (2016) 439–443.
[17] A. Nabi, Compu. Mater. Sci. 112 (2016) 210–218.
[18] X.D. Liu, T. Xing, Solid Stat. Commun. 187 (2014) 72–76.
[19] L.J. Sham, M. Schlüter, Phys. Rev. Lett. 51 (1983) 1888–1891.
[20] J.G. Yu, P. Zhou, Q. Li, Phys. Chem. Chem. Phys. 15 (2013) 12040–12047.
[21] P. Maxwell, Á.M. Pendás, P.L.A. Popelier, Phys. Chem. Chem. Phys. (2016), http://dx.doi.org/10.1039/C5CP07021J.
[22] M.D. Ganji, S.M. Hosseini-khah, Z. Amini-tabar, Phys. Chem. Chem. Phys. 17 (2015) 2504–2511.
[23] J. Yin, X. Lu, Nanosci. Nanotechn. Lett. 7 (2015) 1–6.